

The missing odderon

A. Donnachie^{1,a}, H.G. Dosch^{2,b}, O. Nachtmann^{2,c}

¹ School of Physics and Astronomy, University of Manchester, Manchester M13 9PL, U.K.

² Institut für Theoretische Physik, Universität Heidelberg, Philosophenweg 16, 69120 Heidelberg, Germany

Received: 18 August 2005 / Revised version: 30 September 2005 /

Published online: 5 January 2006 – © Springer-Verlag / Società Italiana di Fisica 2006

Abstract. In contrast to theoretical expectations, experimental results at $\sqrt{s} = 200$ GeV for the reaction $\gamma p \rightarrow \pi^0 X$ show no evidence for odderon exchange. The upper limit on the cross section is an order of magnitude smaller than the theoretical estimate. It is argued that chiral symmetry leads to a large suppression, taking the theoretical estimates well below the data. Two additional arguments are presented which may decrease the theoretical estimate further. The calculations are more sensitive to the assumptions made in evaluating the hadronic scattering amplitude than in the processes considered previously and lattice gauge calculations indicate that the odderon intercept may be appreciably lower than usually assumed. These two latter effects are particularly relevant for the reactions $\gamma p \rightarrow f_2^0(1270)X$ and $\gamma p \rightarrow a_2^0(1320)X$ for which the data upper limits are also below the theoretical predictions, but not so dramatically as for $\gamma p \rightarrow \pi^0 X$.

1 Introduction

The phenomenological pomeron has long been established as an effective Regge pole with trajectory $\alpha_{\text{pom}} \approx 1.08 + 0.25t$ whose exchange governs high-energy diffractive scattering [1]. There is no a priori reason why the phenomenological odderon, a $C = P = -1$ partner of the $C = P = +1$ pomeron, should not exist [2]. Indeed within perturbative QCD, the odderon is rather well defined with an intercept $\alpha_{\text{odd}}(0) \approx 1$ [3]. For a general review of odderon physics see [4]. Applications in the non-perturbative regime [5] have assumed a “maximal” odderon with an intercept $\alpha_{\text{odd}}(0) = 1$. The exchange of the phenomenological odderon should produce a difference between pp and $\bar{p}p$ scattering at high energy and small momentum transfer, a particularly sensitive test being provided by the forward real part of the pp and $\bar{p}p$ scattering amplitudes. However, measurements [6] are consistent with the absence of odderon exchange and rule out the maximal odderon of [5], but not necessarily models in which the forward real part vanishes at large energy; see [7] for example. Another explanation is provided [8] by the clustering of two quarks to form a small diquark in the nucleon which has the effect of suppressing the odderon– N – N coupling and completely so for a point-like diquark. However if one (or both) of the nucleons is transformed into an excited negative-parity state then the odderon can couple without any restriction according to [8]. In contrast to the apparently “missing odderon” at very

small momentum transfers there is experimental evidence for $C = -1$ exchange at larger momentum transfers. The pp and $\bar{p}p$ differential cross sections [9] differ markedly for $|t| \approx 1.3$ GeV² in the ISR energy range. For still larger $|t|$ the $C = -1$ exchange is even supposed to dominate. We shall discuss these two points in Sect. 4 below.

As an alternative to pp and $\bar{p}p$ scattering it was suggested [10, 11] that high-energy photoproduction of $C = +$ mesons, e.g. π^0 , $f_2^0(1270)$ and $a_2^0(1320)$, with nucleon excitation would provide a clean signature for odderon exchange. Specific calculation [12, 13] predicted the following cross sections at $\sqrt{s} = 20$ GeV:

$$\begin{aligned}\sigma(\gamma p \rightarrow \pi^0 X) &\approx 300 \text{ nb}, \\ \sigma(\gamma p \rightarrow f_2^0(1270)X) &\approx 21 \text{ nb}, \\ \sigma(\gamma p \rightarrow a_2^0(1320)X) &\approx 190 \text{ nb}.\end{aligned}\quad (1)$$

The experimental results at $\sqrt{s} = 200$ GeV for π^0 [14], $f_2(1270)$ and $a_2(1320)$ [15] are

$$\begin{aligned}\sigma(\gamma p \rightarrow \pi^0 N^*) &< 49 \text{ nb}, \\ \sigma(\gamma p \rightarrow f_2^0(1270)X) &< 16 \text{ nb}, \\ \sigma(\gamma p \rightarrow a_2^0(1320)X) &< 96 \text{ nb},\end{aligned}\quad (2)$$

all at the 95% confidence level. The model was based on an approach to high-energy diffractive scattering using functional integral techniques [16] and an extension [17] of the model of the stochastic vacuum [18]. This model gives a remarkably good description of many different processes dominated by pomeron exchange [17, 19]. It is easily extended to odderon exchange and gives an odderon intercept

^a e-mail: sandy.donnachie@manchester.ac.uk

^b e-mail: h.g.dosch@thphys.uni-heidelberg.de

^c e-mail: o.nachtmann@thphys.uni-heidelberg.de

$\alpha_{\text{odd}}(0) = 1$. The scattering amplitude $T(s, t)$ is obtained through a profile function $J(\mathbf{b}, s)$:

$$T(s, t) = 2is \int d^2b \exp(i\mathbf{q} \cdot \mathbf{b}) J(\mathbf{b}, s). \quad (3)$$

The function $J(\mathbf{b}, s)$ is given in turn by the overlap of a dipole–dipole scattering amplitude $\tilde{J}(\mathbf{b}, \mathbf{r}_1, \mathbf{r}_2, z_1, z_2)$ with appropriate wave functions for the initial and final states:

$$J(\mathbf{b}, s) = - \int \frac{d^2r_1}{4\pi} dz_1 \int \frac{d^2r_2}{4\pi} dz_2 \\ \times \sum \Psi_M^*(\mathbf{r}_1, z_1) \Psi_\gamma(\mathbf{r}_1, z_1) \Psi_p^*(\mathbf{r}_2, z_2) \Psi_p(\mathbf{r}_2, z_2) \\ \times \tilde{J}(\mathbf{b}, \mathbf{r}_1, \mathbf{r}_2, z_1, z_2), \quad (4)$$

where the sum corresponds to a summation over the flavour and spin indices of the constituents in the wave functions and the summation over the nucleon resonances and their spins is implied in the cross section. In (4), \mathbf{b} is the impact parameter of two light-like dipole trajectories with transverse sizes \mathbf{r}_1 and \mathbf{r}_2 respectively and z_1, z_2 are the longitudinal momentum fractions of the quarks in the dipoles. The physical picture is that the photon fluctuates into a $q\bar{q}$ pair; this is turned into the final meson M by the soft-colour interaction \tilde{J} , determined from other reactions [19] and the proton is excited into an appropriate baryon resonance. The nucleon and the baryon resonances are treated as quark–diquark dipole systems. The wave functions automatically take into account helicity flip at the particle and at the quark level and produce the correct helicity dependence of $d\sigma/dt$ as $t \rightarrow 0$ for Regge-pole exchange. The cross sections for π^0 , $f_2^0(1270)$ and $a_2^0(1320)$ photoproduction were evaluated at $\sqrt{s} = 20$ GeV as that is the energy at which the parameters of $\tilde{J}(\mathbf{b}, \mathbf{r}_1, \mathbf{r}_2, z_1, z_2)$ were obtained. In elastic hadron–hadron scattering the increase of the cross sections, together with the shrinking of the diffractive peak, can be reproduced in this model by suitable scaling of the hadronic radii. The assumption that the same radial scaling is relevant for the energy dependence of the odderon contributions, leads to the photoproduction cross sections scaling as $(\sqrt{s}/20)^{0.3}$ and to an enhancement of about 2 at $\sqrt{s} = 200$ GeV.

The results for diffractive dissociation depend much more on the choice of wave functions than for elastic processes. In the latter the overlap is essentially the density and is constrained by the normalisation, which is not the case for the former. The photon–meson overlap is tested to some extent by the known radiative decays of the meson, but there is no such test for the overlap between the proton and the final baryonic state. Also, the odderon exchange is much more sensitive to the parameters of the model than is pomeron exchange; see Sect. 3 below. For these reasons it was suggested [12, 13] that the uncertainty in the model calculation is at least a factor 2 at $\sqrt{s} = 20$ GeV.

The results (2) are well below the predictions (1), for the π^0 drastically so. Thus, from pp and $\bar{p}p$ scattering as well as from meson production one concludes that the odderon is apparently “missing” at small $|t|$. It is important to understand why this may be so. In the following we reconsider each part of the calculations of [12, 13].

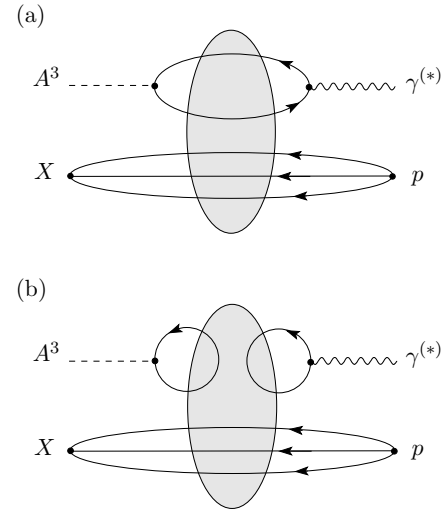


Fig. 1. Diagrams of type **a** and **b** for the process $\gamma^{(*)}p \rightarrow A^3 X$. The full lines correspond to quark propagators in a given gluon potential. The shaded blobs indicate the functional integration over all gluon potentials with a measure including the fermion determinant. For the process $\gamma^{(*)}p \rightarrow \gamma^{(*)}p$ replace A^3 by $\gamma^{(*)}$ and X by p

2 Wave functions

Consider first π^0 photo- and electroproduction at high energies,

$$\gamma^{(*)}(q) + p(p) \rightarrow \pi^0(q') + X(p'), \quad (5)$$

where X is a proton or a diffractively-excited proton state. We shall argue that chiral $SU(2) \times SU(2)$ symmetry of QCD, which is broken only by the small u and d quark masses, leads to a large suppression factor for this reaction. A detailed account of this will be given in [20]. Here we only outline the arguments.

Real and virtual Compton scattering,

$$\gamma^{(*)}(q) + p(p) \rightarrow \gamma^{(*)}(q') + p(p'), \quad (6)$$

were investigated in [21, 22] using exact functional techniques. A classification of diagrams into seven types a to g (see Fig. 2 of [21]) was given. The diagrams of types a and b, which are the relevant ones for our discussion here, are as shown in Fig. 1 of the present paper with A^3 replaced by $\gamma^{(*)}$ and X by p . The diagram types are distinguished by the topology of the quark loops and the placing of the photon coupling on them. It was argued in [21, 22] that at high energies the diagrams of types a and b are the leading ones.

Now one can use PCAC (partial conservation of the axial current) to relate reaction (5) to a process very similar to (6) where the final state $\gamma^{(*)}$ is replaced by the third isospin component of the axial current, A_μ^3 , and the final state proton by X :

$$\gamma^{(*)}(q) + p(p) \rightarrow A^3(q') + X(p'). \quad (7)$$

The isotriplet of axial currents is

$$A_\mu^a(x) = \bar{q}(x) \gamma_\mu \gamma_5 \frac{\tau^a}{2} q(x), \quad (8)$$

where $a = 1, 2, 3$, τ^a are the Pauli matrices and

$$q(x) = \begin{pmatrix} u(x) \\ d(x) \end{pmatrix} \tag{9}$$

is the quark field operator. The well-known PCAC relation is

$$\partial_\lambda A^{a\lambda}(x) = \frac{f_\pi m_\pi^2}{\sqrt{2}} \phi^a(x), \tag{10}$$

where $\phi^a(x)$ is a correctly normalised pion field and $f_\pi \cong 0.93m_\pi$ is the pion decay constant. By PCAC the amplitudes of the reactions (5) and (7) are related by

$$\begin{aligned} & iq'_\mu \mathcal{M}^{\mu\nu}(A^3; q', p, q) \\ &= -\frac{f_\pi m_\pi^2}{2\pi m_p \sqrt{2}} \frac{1}{q'^2 - m_\pi^2 + i\epsilon} \mathcal{M}^\nu(\pi^0; q', p, q). \end{aligned} \tag{11}$$

Here m_p is the proton mass and we extrapolate the amplitude for (5) from on shell pions, $q'^2 = m_\pi^2$, to arbitrary $q'^2 \leq m_\pi^2$. One can then show the following: At high energies the diagrams of types a and b shown in Fig. 1 are the leading ones for reaction (7).

For simplicity we discuss in this note only the isospin-symmetry limit, that is we set for the current quark masses

$$m_u = m_d \equiv \hat{m}. \tag{12}$$

The quark loop attached to the current A^3_μ in Fig. 1b must then vanish, since τ^3 is the only non-trivial flavour matrix in this loop and $\text{tr}\{\tau^3\} = 0$. Thus we find: In the isospin-symmetry limit the diagrams of type b vanish for the reaction (7) and, using (11), also for pion production (5).

A more involved analysis is necessary for the diagrams of type a. Using PCAC (10) one can show the following [20]: The diagrams of type a when inserted in (11) give a contribution to the π^0 amplitude which is proportional to \hat{m} , that is to the current quark mass.

The current quark mass is proportional to m_π^2 in the chiral limit (see for instance (8.1) of [23])

$$m_\pi^2 = 2\hat{m}B, \quad B = -\frac{2}{f_\pi^2} \langle 0|\bar{u}u|0\rangle. \tag{13}$$

Typical values for \hat{m} and B at a renormalisation scale of 1 GeV are $\hat{m} = 7\text{ MeV}$, $B = 1.4\text{ GeV}$.

Thus we find that the amplitude for (5) is proportional to m_π^2 , that is it vanishes in the chiral limit. To estimate the actual suppression factor κ in the amplitude relative to a naive estimate, such as the one given in [12], we argue as follows. To get a dimensionless factor we divide m_π^2 by a typical hadronic squared mass scale, say m_p^2 , and write

$$\kappa = \frac{m_\pi^2}{m_p^2} h. \tag{14}$$

Here h should be of order 1 but could be numerically large, for instance $h = m_p/f_\pi \cong 7$. Putting everything together we estimate for the suppression factor

$$0.02 \lesssim \kappa \lesssim 0.15,$$

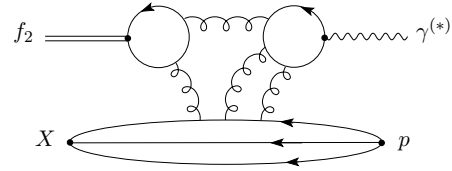


Fig. 2. A specific diagram of type b for $\gamma^{(*)}p \rightarrow f_2^0 X$

$$5 \times 10^{-4} \lesssim \kappa^2 \lesssim 0.02. \tag{15}$$

That is, the cross section for $\gamma p \rightarrow \pi^0 X$ should be suppressed at least by a factor ≈ 50 .

Thus one shortcoming of the calculation [12] for $\gamma p \rightarrow \pi^0 X$ is that the π^0 wave function used did not properly take into account the constraints from chiral symmetry. This clearly reduces the theoretical prediction for (5). Of course, other effects, as discussed in this note, may reduce the theoretical estimate further.

What can we say about f_2^0 and a_2^0 production? We note that the $f_2^0(1270)$ is an isoscalar, the $a_2^0(1320)$ an isovector particle. One can again make a general analysis in terms of diagram types, replacing A^3 in Fig. 1 by appropriate tensor currents. Here we only note that in the isospin-symmetry limit the same arguments as given for the A^3_μ case above show that diagrams of type b cannot contribute to $\gamma^{(*)}p \rightarrow a_2 X$ but can contribute to $\gamma^{(*)}p \rightarrow f_2^0 X$. A simple diagram of this type is shown in Fig. 2. Thus, if for some reason diagrams of type a in Fig. 1 are suppressed also for tensor meson production, then a_2^0 will be suppressed but f_2^0 need not be. Data [15] may give a hint in this direction.

3 Soft-colour interaction

The functional approach to quantum field theory has turned out to be a most effective one for investigating non-perturbative effects in QCD. In it the expectation values of field operators are expressed as functional integrals over the classical fields, where the weight of the configuration is given by the exponential of the QCD action. This functional integration takes into account the quantum fluctuations. The short-range fluctuations can be calculated with the help of perturbation theory, but for a treatment of the effects of long-range fluctuations numerical simulations or model assumptions are necessary.

The stochastic vacuum model (for a review see [24]) is one such approach to non-perturbative QCD. It assumes that the long-range fluctuations can be approximated by the only functional integral which is analytically accessible, namely a Gaussian functional integral (Gaussian process). The Gaussian approximation is defined through the cumulant or linked-cluster expansion [25] of the expectation value of several fields. If all cumulants containing more than two fields are neglected we are left with Gaussian integrals and all expectation values can then be expressed through products of the expectation value of two fields, the so-called correlator.

In a theory where the variables of the functional integration, that is the classical fields, commute, the Gaussian approximation is uniquely defined. In a non-Abelian field

theory this is not the case, since there are several cumulant expansions possible and the truncation of them leads to different Gaussian approximations. An additional complication is induced by the dependence on the path connecting the space-time points of the two fields of the correlator. This path has to be introduced in order to ensure gauge independence.

For the investigation of the forces between two quarks and in particular for confinement, the expectation value of a single Wilson loop has to be calculated. In that case the so-called van Kampen cumulants are a natural choice for the expansion and the truncation of it leads to a Gaussian integral. This allows the approximate evaluation of expectation values of a single Wilson loop. This choice, together with the assumption that the paths mentioned above have no influence on the correlator, led to several highly desirable results [24]. In particular we see the following.

- (1) A non-Abelian gauge theory like QCD shows confinement. In order to obtain confinement in an Abelian gauge theory monopole condensation has to occur.
- (2) When lattice results for the fundamental correlator are inserted, the string tension comes out to have the correct phenomenological value. Furthermore it is proportional to the Casimir operator of the representation of the Wilson loop, a result which is also in good agreement with lattice calculations.

These results support strongly the Gaussian approximation. Also the relativistic spin- and velocity-dependent terms of the interquark potential, as obtained from the model, are in agreement with phenomenology.

In order to evaluate hadronic scattering amplitudes the expectation value of at least two Wilson loops has to be calculated [17]; this follows from the formalism developed in [16]. However the functional integration variables in the expansion used for the evaluation of one loop cannot be used in that case. Therefore two new different cumulant expansions have been used, a simple expansion method and a more sophisticated super-cumulant method, as explained in detail in Chapt. 8.5 of [1]. Both these cumulant expansions differ from the one used for the evaluation of a single loop. Hence the Gaussian approximations made for the single loop and that made for scattering processes are not the same. The details are discussed in [24, 26, 27].

Nevertheless the modified model with the same input parameters for the correlator gives very satisfactory results for scattering and production processes where pomeron exchange is dominant. With only a few parameters a whole range of experimental results could be reproduced and even predicted [1, 19]. The model can also be applied to processes which can only occur via the exchange of a C -odd state, for instance the photoproduction of neutral pions, and is at the core of the predictions of [12, 13]. The fact that the predicted cross section for $\gamma p \rightarrow \pi^0 X$ is an order of magnitude larger than the upper limit of the experimental cross section for this reaction forces us to consider possible sources of error in the extended stochastic vacuum model. It was already mentioned that the underlying cumulant expansions used for the evaluation of scattering amplitudes are different from those used for the evaluation of one loop. For definiteness we call the cumulants of the latter

W-cumulants and those of the former S-cumulants (for scattering). Only the correlator (the cumulant of two fields) is the same in all expansions. The vanishing of the higher W-cumulants does not imply the vanishing of the higher S-cumulants.

Scattering processes with pomeron (C -even) exchange are dominated by the expectation value of a product of four gluon fields that is reduced to the product of two correlators. The success of the model for these processes shows that the cumulant of four fields is indeed not only small for the W- but also for the S-expansions. For C -odd induced processes the leading term is the expectation value of a product of six fields. In the model it is factorised to a product of three correlators. This factorisation is only justified if additionally the S-cumulant for six fields is small. It should be noted that the two S-expansions mentioned above do not differ in the cumulant of four fields but do in that of six fields, hence the S-cumulant of six fields cannot vanish in both S-expansions. Thus a possible explanation for the discrepancy between the theoretical expectation (1) and the experiment (2) is a large S-cumulant of six fields compensating the product of the three correlators to a large extent. This is independent from the wave function effects discussed in Sect. 2.

Lattice calculations could provide a test for this hypothesis of a large S-cumulant of six fields [28]. The leading term for the difference between expectation values of a product of parallel and antiparallel Wilson loops is the expectation value of six fields. Comparison between model and full lattice calculations can therefore test directly the factorisation hypothesis without involving the folding with hadron wave functions which always occurs in the evaluation of scattering or production processes.

4 Energy dependence

There is no a priori justification for the assumption that the odderon trajectory should match the pomeron trajectory nor, in particular, that their contributions to elastic processes should have the same energy dependence. There is some evidence that they may indeed be different. The differential cross sections of elastic pp and $\bar{p}p$ scattering at $\sqrt{s} = 53 \text{ GeV}$ are different in the region of $|t| = 1.3 \text{ GeV}^2$, the pp data having a marked dip which is not present in the $\bar{p}p$ data. This difference must be due to $C = -1$ exchange and is the only real experimental evidence for the existence of the odderon. The data can be fitted by including, in addition to the usual pomeron and other Regge poles, the maximal odderon [5] or three-gluon exchange [7] which is closer in spirit to the perturbative odderon than to the non-perturbative odderon of [5] or the odderon of [29]. Indeed, in [29] the odderon contributions to pp and $\bar{p}p$ scattering were calculated treating the impact factors (wave functions) with the same methods discussed above for single-meson photoproduction. The proton was still considered as a quark-diquark system but now the diquark was assumed to have an average size $\langle d \rangle$. It was shown in [29] that for $\langle d \rangle = 0$ the odderon effects in pp versus $\bar{p}p$ at $|t| \approx 1.3 \text{ GeV}^2$ vanish in accordance with [8] and that the data [9] could

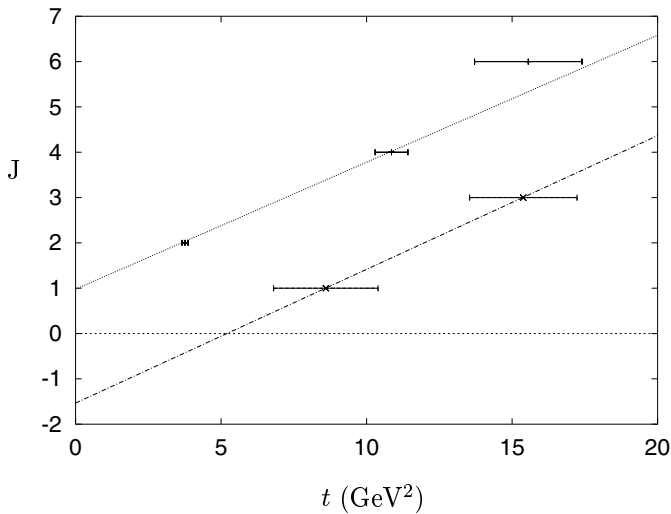


Fig. 3. Pomeron and odderon trajectories from lattice gauge theory. The data points are from [31]

be reproduced with a – very reasonable – average diquark size $\langle d \rangle \approx 0.22$ fm.

The pp data at large $|t|$ appear to be essentially energy independent for $27.4 \leq \sqrt{s} \leq 62.1$ GeV and, in both models [5] and [7], are primarily odderon exchange. If the odderon is considered as a Regge pole then the near-constancy of the pp large- $|t|$ cross section requires the maximal odderon to have a very flat trajectory. See [4] for a full discussion of these points.

However, a rather different picture emerges from lattice gauge theory [30, 31]. In [31], the lightest $J = 0, 2, 4, 6$ glueball masses have been calculated in the $D = 3+1$ $SU(3)$ gauge theory and extrapolated to the continuum limit. Assuming that the masses lie on linear Regge trajectories, the leading glueball trajectory is found to be $\alpha(t) = (0.93 \pm 0.024) + (0.28 \pm 0.02)\alpha'_R t$, where $\alpha'_R \approx 0.9$ is the slope of the usual mesonic Regge trajectories. Thus this glueball trajectory has an intercept and slope very similar to that of the pomeron trajectory, $\alpha_{\text{pom}} \approx 1.08 + 0.25t$ [1]. The states one might expect to lie on the odderon trajectory are the lightest $J^{PC} = 1^{--}, 3^{--}, 5^{--}, \dots$. The lattice results for 1^{--} and 3^{--} define a trajectory with a slope similar to the pomeron but with a very low, negative intercept. These results are shown in Fig. 3. A similar conclusion about the odderon trajectory is reached in [32] but from a very different standpoint. As the glueballs on the pomeron trajectory are two-gluon states and those on the odderon trajectory are three-gluon states, that the latter is low-lying is not surprising in a constituent-gluon picture as the effective gluon mass ~ 1 GeV. If this is the correct interpretation of the lattice calculations, then it completely destroys the odderon exchange model used to calculate π^0 , $f_2^0(1270)$ and $a_2^0(1320)$ photoproduction.

However there is an alternative explanation of the lattice result for the odderon. If the leading trajectory has an intercept around unity then the lightest 1^{--} glueball cannot lie on it but will lie on a subleading trajectory. Drawing a linear trajectory from $J = 1$ at $t = 0$ through the mass of the lightest 3^{--} glueball gives a slope about

half the slope of the pomeron trajectory. The ambiguity would be removed if the mass of the lightest 5^{--} could be calculated. This alternative explanation does not have a significant effect on the calculation of [12, 13].

5 Conclusions

We have presented three arguments highlighting aspects of the predictions [12, 13] for odderon exchange in photoproduction which may have been too optimistic. These are the role of wave functions and in particular the effect of chiral $SU(2) \times SU(2)$ symmetry, the possible breakdown of the factorisation procedures used in calculating the interaction and uncertainties in the energy dependence of odderon exchange. The first of these leads to a large suppression for the reaction $\gamma^{(*)}p \rightarrow \pi^0 X$ and can account for the large discrepancy between the data [14] and the original predictions. The other two aspects of the calculation are less quantifiable, but could provide an explanation of the discrepancies between prediction and experiment in the reactions $\gamma p \rightarrow f_2^0(1270)X$ and $\gamma p \rightarrow a_2(1320)X$. Both the factorisation procedure and the assumption on energy dependence are amenable to being checked by lattice gauge calculations.

Acknowledgements. We are grateful to C. Ewerz for providing Figs. 1 and 2. We have greatly profited from comments on the manuscript by C. Ewerz, H.Ch. Schultz-Coulon, and A. Utermann. Discussions with K.H. Meier, H.Ch. Schultz-Coulon and J. Stiewe are gratefully acknowledged. This work was supported in part by the German Bundesministerium für Bildung und Forschung under project no. HD 05HT4VHA/0.

References

1. A. Donnachie, H.G. Dosch, P.V. Landshoff, O. Nachtmann, Pomeron physics and QCD (Cambridge University Press 2002)
2. L. Lukaszuk, B. Nicolescu, Nuov. Cim. Lett. **8**, 405 (1973); D. Joynson, E. Leader, C. Lopez, B. Nicolescu, Nuov. Cim. A **30**, 345 (1975); B. Nicolescu in Protvino 1999, Elastic and diffractive scattering, edited by V.A Petrov, A.V. Prokudin (World Scientific, Singapore 2005) [hep-ph/9911334]
3. R.A. Janik, J. Wosiek, Phys. Rev. Lett. **82**, 1092 (1999); J. Bartels, L.N. Lipatov, G.P. Vacca, Phys. Lett. B **477**, 178 (2000)
4. C. Ewerz, The Odderon in Quantum Chromodynamics, hep-ph/0306137
5. P. Desgrolard, M. Giffon, E. Predazzi, Z. Phys. C **63**, 241 (1994)
6. N.A. Amos et al., E710 Collaboration, Phys. Rev. Lett **68**, 2433 (1992); C. Augier et al., UA4/2 Collaboration, Phys. Lett. B **316**, 448 (1993)
7. A. Donnachie, P.V. Landshoff, Nucl. Phys. B **267**, 690 (1986)
8. M. Rueter, H.G. Dosch, Phys. Lett. B **380**, 177 (1996)
9. A. Breakstone et al., Phys. Rev. Lett. **54**, 2180 (1985)

10. A. Schäfer, L. Mankiewicz, O. Nachtmann, in Workshop on Physics at HERA 1991, edited by W. Buchmüller, G. Ingelman, DESY (1992); W. Kilian, O. Nachtmann, *Eur. Phys. J. C* **5**, 317 (1998)
11. V.V. Barahovsky, I.R. Zhitnitsky, A.N. Shelkovenko, *Phys. Lett. B* **267**, 532 (1991)
12. E.R. Berger et al., *Eur. Phys. J. C* **9**, 491 (1999)
13. E.R. Berger, A. Donnachie, H.G. Dosch, O. Nachtmann, *Eur. Phys. J. C* **14**, 673 (2000)
14. C. Adloff et al., H1 Collaboration, *Phys. Lett. B* **544**, 35 (2002)
15. T. Berndt (for the H1 Collaboration), *Acta Phys. Polonica B* **33**, 3499 (2002)
16. O. Nachtmann, *Ann. Phys.* **209**, 436 (1991)
17. A. Krämer, H.G. Dosch, *Phys. Lett. B* **272**, 114 (1991); H.G. Dosch, E. Ferreira, A. Krämer, *Phys. Lett. B* **289**, 153 (1992)
18. H.G. Dosch, *Phys. Lett. B* **190**, 177 (1987); H.G. Dosch, Yu.A. Simonov, *Phys. Lett. B* **205**, 339 (1988)
19. H.G. Dosch, E. Ferreira, A. Krämer, *Phys. Rev. D* **50**, 1992 (1994); E. Ferreira, F. Pereira, *Phys. Rev. D* **55**, 130 (1997); H.G. Dosch, T. Gousset, G. Kulzinger, H.J. Pirner, *Phys. Rev. D* **55**, 2602 (1997); E. Ferreira, F. Pereira, *Phys. Rev. D* **56**, 179 (1997); H.G. Dosch, T. Gousset, H.J. Pirner, *Phys. Rev. D* **57**, 1666 (1998); M. Rueter, H.G. Dosch, *Phys. Rev. D* **57**, 4097 (1998); G. Kulzinger, H.G. Dosch, H.J. Pirner, *Eur. Phys. J. C* **7**, 73 (1999); E. Berger, O. Nachtmann, *Eur. Phys. J. C* **7**, 459 (1999)
20. C. Ewerz, O. Nachtmann, to be published
21. C. Ewerz, O. Nachtmann, Towards a Nonperturbative Foundation of the Dipole Picture. I: Functional methods, hep-ph/0404254
22. C. Ewerz, O. Nachtmann, Towards a Nonperturbative Foundation of the Dipole Picture: II. High Energy Limit, to be published
23. J. Gasser, H. Leutwyler, *Phys. Rep.* **87**, 77 (1982)
24. A. Di Giacomo, H.G. Dosch, V.I. Shevchenko, Yu.A. Simonov, *Phys. Rep.* **372**, 319 (2002)
25. N.G. van Kampen, *Phys. Rep. C* **24**, 172 (1976)
26. M. Rueter, H.G. Dosch, *Z. Phys. C* **66**, 245 (1995)
27. O. Nachtmann, in *Perturbative and Nonperturbative Aspects of Quantum Field Theory*, edited by H. Latal, W. Schweiger (Springer, Berlin, Heidelberg 1997)
28. A.I. Shoshi, F.D. Steffen, H.G. Dosch, H.J. Pirner, *Phys. Rev. D* **68**, 074004 (2003)
29. H.G. Dosch, C. Ewerz, V. Schatz, *Eur. Phys. J. C* **24**, 561 (2002) [hep-ph/0201294]
30. C.J. Morningstar, M.J. Peardon, *Phys. Rev. D* **60**, 034509 (1999)
31. H.B. Meyer, M.J. Teper, *Phys. Lett. B* **605**, 344 (2005)
32. Yu.A. Simonov, A.B. Kaidalov, *Phys. Lett. B* **477**, 163 (2000)